Preprint

UCRL-JC-152969

Effect of Humidity During the Coating of Stöber Silica Sols

T. Suratwala*, M. L. Hanna, P. Whitman

This article was submitted to Journal of Non-Crystalline Solids

07-14-03

U.S. Department of Energy

Lawrence
Livermore
National
Laboratory

DISCLAIMER

Submit: Journal of Non-Crystalline Solids

Effect of humidity during the coating of Stöber silica sols

T. Suratwala*, M. L. Hanna, P. Whitman
Lawrence Livermore National Laboratory, P.O. Box 808, Livermore, CA 94551, USA

Keywords: Sol gel, spin coating, dip coating, anti-reflection, high-peak-power lasers, colloidal silica, capillary condensation, microcracking, refractive index, National Ignition Facility

Abstract

Various silica sols (varying in surface chemistry and solvent) were synthesized by the Stöber process and then subsequently coated on substrates at various humidities. For ethanol-based sols, films prepared at low humidities had a higher refractive index, lower thickness, and greater microcracking than those prepared at high humidities. The change in film properties followed an abrupt, instead of a gradual, change with humidity. This change in film microstructure can be explained by the ability/inability of capillary condensed water in the micropores of the colloid to evaporate and to collapse the micropores. The magnitude of the shrinkage and the relative humidity at which the pores collapsed were found to depend on the colloid surface chemistry and the coating method. In contrast to the ethanol-based sols, humidity during spin coating had a negligible effect on film properties for sec-butanol and decane -based sols. This is likely due to the lower vapor pressure and/or lower water solubility of these solvents such that the pores in the latter stages of drying the films did not contain much water. Understanding this behavior has been important for improving the performance and process repeatability of using these films as anti-reflective coatings in high-peak-power laser systems.

*Corresponding author. Tel.: +1-925 422 1884; fax +1-925 423 0792. E-mail address: suratwala1@llnl.gov (T.I. Suratwala).

1. Introduction

Anti-reflection (AR) silica coatings prepared by the sol-gel process have been and are being used on transmissive optical components of high-powered fusion lasers, such as NOVA, OMEGA, and the National Ignition Facility (NIF) [1,2]. These AR coatings have high damage thresholds, 2-3 times that of other coating materials [3], which makes them particularly attractive for use in such laser systems.

The coating solutions are monodisperse silica sols (typically 20 nm in diameter), made by a sol-gel route called the Stöber process developed more than 30 years ago [4]. In the Stöber process, silica particles are created by the hydrolysis and condensation of silicon alkoxides in alcohol solvents in the presence of H_2O and a base (e.g., ammonia). The films, which are prepared by spin or dip coating the sols, are essentially a random stacking of silica colloids on the optical surface. The highly porous nature of these films provides the low refractive index needed for anti-reflection.

In our previous studies, various types of silica sol coating solutions were developed having different surface chemistries, solvents, and porosities such that they can: (1) be tailored for different optical substrates, (2) provide improved coating behavior over large areas, (3) have long term stability, and (4) have resistance to moisture and organic contaminants in the use environment [1,5,6]. For the NIF, over 5000 large optics (0.5–1 m in size) need to be AR coated. Coating uniformity and repeatability are needed, specifically with respect to refractive index and thickness, which determine the AR performance.

In other studies, various aspects of sol-gel thin film formation have been examined, such as the effects of: (1) size and structure of silicate species, (2) the relative rates of evaporation and condensation, and (3) magnitude of capillary pressure and shear stresses on film properties (namely, film thickness and porosity) [7-9]. In this study, we examine the effect of humidity of the environment during film preparation. A series of different sols synthesized by the Stöber process, having different solvents and surface chemistries, are coated by either spin or dip coating at various humidities at room temperature. We find that the humidity during coating can strongly affect the refractive index and thickness of the final coating, and therefore its AR properties.

2. Experimental

Preparation of sols. A series of standard sol solutions used to make AR coating for NIF optics were prepared. The details of the preparation of the sols and their properties can be found elsewhere [5,6]. All of the sols contain nominally 20 nm particles and they differ in solvent and/or the surface chemistry of the colloids (see Tables 1 & 2).

Spin Coating. Approximately 1 ml of sol was dropped onto a spinning (1500-2400 rpm) 2 inch Si wafer, and the coating was allowed to spread and dry for ~2 min. The spinning rate was adjusted for each sol to maintain a thickness of ~200 nm for the low humidity coating. Note the same spin rate was used for a single sol type (listed in Table 1) regardless of the humidity. The spin coating chamber was sealed in a plastic box with a small cover, and the humidity in the chamber was controlled by flowing a mixture of dry N_2 gas and water-saturated N_2 gas prepared by bubbling through room temperature

water. The humidity was measured using a humidity sensor (Testo 625 hygrometer), and all the coatings were prepared at room temperature (22^{o}C).

Dip Coating. The sol to be coated was placed in a 500 ml beaker. This beaker was placed inside a 2-L beaker equipped with a lid with a slit, and a tubing was inserted into the bottom of the large beaker. N_2 at fixed humidity (prepared in same manner as described above) was flowed through the tube. Clean 2-inch Si wafers were dipped vertically in the sol for 10 minutes and then drawn out at a specific draw rate that would give the desired thickness. For example, the draw rate for Sol A was 7 cm/min. The wafers were allowed to hang over the sol for 5 minutes and then removed from the coating chamber.

Ellipsometry. The refractive index at 633 nm and the thickness of the films were determined by spectroscopic ellipsometry in a dry environment. Details of this measurement are described elsewhere [5].

Nitrogen Adsorption Measurements and Scanning Electron Microscopy. The sols were air dried at room temperature to form a powder and then vacuum dried at 80^{o}C for 24-48 hrs. Nitrogen adsorption was measured. The particles surface area was calculated using Brunauer-Emmet-Teller (BET) model [10] and the microporosity was calculated using t-plot analysis [11]. Secondary scanning electron microscopy (Hitachi SEM) was performed on top surface of as-prepared sol films.

3. Results

3.1 Index and Thickness

Table 2 lists the measured refractive index and thickness of the various sols spin-coated at 14% and 60% RH. The films prepared from ethanol-based sols show a higher index and a lower film thickness when coated at low humidity, compared to those coated at high humidity. However, the last two sols listed in Table 2 (in sec-butanol or decane) showed little change in film properties with change in humidity.

Two of the ethanol-based sols (Sol A and Sol B), because they showed the greatest change in film properties, were examined in more detail. The index and thickness of these films are plotted as a function of humidity during spin coating in Figs. 1a & b. Again, the films prepared at low humidities had a higher index and lower thickness than those prepared at high humidities. Notice that film properties change abruptly over a narrow humidity range (at ~35-40% RH for the Sol A (Fig. 1a) and at ~25% RH for the Sol B (Fig. 1b)).

A similar humidity effect on index and thickness was also observed when the films were prepared by dip coating. Those results for Sol A are shown in Fig. 2. Notice that magnitude of the index change and thickness change was greater for the samples prepared by spin coating (Fig. 1a) than by dip coating (Fig. 2). Also, the humidity at which the abrupt change in index and thickness was observed is different; 35-40% RH for spin coating and 45-50% RH for dip coating.

3.2 Microstructure

Figure 3 shows an SEM image of one of the films prepared from Sol A. This image shows that the coatings are just the random stacking of silica particles ~20nm in size. Figure 4 shows SEM images viewed from the top for three different sols coated at low humidity (left side) and high humidity (right side). Films prepared from Sols A and B (in ethanol) showed much less microcracking when coated at high humidities. In contrast, the films prepared from Sol E (in decane) did not show any difference in amount of microcracking. The presence of microcracking indicates that the coating had experienced shrinkage in the final stages of drying.

3.3 Ammonia treatment

Many of the AR coatings used on silica optics for NIF are vapor ammonia treated, because it provides a more mechanically stable coating and a lower microporosity coating [5]. Two of the prepared films from Sol A were ammonia vapor treated at room temperature for 16 hrs and the properties were remeasured. Details of the ammonia treatment procedure can be found elsewhere [5]. The results for index and thickness are shown in Fig. 5. Ammonia vapor treatment is known to densify the sol coating and remove remaining micropores in the colloid [12]. The key result observed in Fig. 5 is that the final index and thickness will vary significantly even after ammonia treatment when humidity during spin coating is varied. The sol coated at low humidity had a final index and thickness of 1.243 and 1660 Å and the sol coated at high humidity had a final index and thickness of 1.178 and 2070 Å. Sols coated at low humidities appear to shrink much more than the sols coated at high humidities even after ammonia treatment. The large differences in microstructure of two ammonia treated films are illustrated in Fig. 6.

4. Discussion

4.1 Coating mass and optical path length

The spin coating process has been described as a four-stage process [13]: (1) deposition; (2) spin-up; (3) spin-off; and (4) evaporation. During the deposition stage, the coating solution is delivered to the substrate. During spin-up, the solution covers the entire substrate due to centrifugal force generated by the rotating substrate. In the Spin-off stage, the excess liquid flows (also driven by centrifugal force) radially and flies off the edge, typically resulting in a wet film of nearly uniform thickness. At the end of the Spin-off stage, the stagnation point (no further solid particles are removed from the substrate) is reached [8]. In other words, the stagnation point help defines the final dried mass of the coating. Evaporation of the solvent(s) occurs throughout all the stages in the coating process. The rate of evaporation depends on two factors: 1) partial pressure difference of the solvent(s) between the surface layer of coating and gas flow just above; and 2) convective and diffusive transport of the vaporized solvents away from the coating area.

To verify that the effects of the humidity on the coating properties happens after the stagnation point, we calculate the areal mass (m_f) ($\mu g/cm^2$) of the coating in terms of the volume fraction solids (f_{SiO2}) as:

$$m_f = t_f f_{SiO_2} \rho_{SiO_2} \quad (1)$$

where t_f is the measured thickness of the final coating and ρ_{SiO2} is the density of dense-amorphous silica (2.2 gm/cm^3). The volume fraction solids can be calculated from the measured film refractive index (n_f) using a simple composite model for the film index:

$$n_f = n_{SiO_2} f_{SiO_2} + n_{air} (1 - f_{SiO_2}) \quad (2)$$

where n_{SiO2} is the index of dense-amorphous SiO_2 (1.46) and n_{air} is the index of air (1.00). Take, for example, the films made from the Sol A (Fig. 1a). The calculated areal mass (using Eqs. 1 & 2) is essentially constant at ~20 $\mu g/cm^2$, regardless of the humidity in which the films were prepared (Fig. 7). This verifies that the changes in coating properties are occurring after the stagnation point. In other words, the observed index and thickness change is solely a change in the packing and/or porosity of the colloids.

The effectiveness of a single layer/ single wavelength AR coating is determined by how close the optical path length (OPL) of the coating matches $\lambda/4$, where λ is the wavelength of light of interest. The OPL is determined by both the film thickness and index:

$$OPL = n_f t_f . \quad (3)$$

The OPL was found not to be constant; it was a function of humidity during spin coating; Fig. 7 shows how the OPL is noticeably higher at higher humidities. Hence, the change in OPL could lead to a noticeable change in AR properties of NIF optics. Effect of humidity on AR coating performance is described in greater detail in Section 4.4.

4.2 Capillary condensation and the relative rates of evaporation & condensation

Shrinkage can continue beyond the stagnation point due to capillary pressures exhorted upon solvent removal from the pores in the coating. The amount of shrinkage that takes place will be governed by the relative rates of evaporation of the solvent and of condensation of the silica matrix [14,15]. Sol-gel derived silica sols typically contain colloids that are very porous in nature, and these colloids have a siloxane network that is incomplete both at the surface and within the colloids. The inorganic polymerization (condensation) reaction, which is given by:

$$\equiv Si - OR \quad + \quad \equiv Si - OR' \quad \rightarrow \quad \equiv Si - O - Si \equiv \quad + \quad ROR' \quad (4)$$

where R and R' are either H or CH_2CH_3, can proceed during the coating process. This reaction is both concentration and pH dependent [16]. As the condensation increases, the coating gains strength. Shrinkage will only occur when capillary pressure caused by evaporation exceeds the strength of the film.

As discussed in the Results section, the thickness and refractive index of the final coating, as well as the amount of microcracking, were found to abruptly change with humidity in the environment during the coating process. All the colloidal solutions used in the present study initially contain 0.25-1.0 vol% H_2O in the solution (see Table 2); hence it is unlikely that moisture in the environment is strongly affecting the

condensation rate (Eq. 4). However, the humidity does strongly influence the partial pressure difference of H_2O between the wet coating surface and the atmosphere (i.e, H_2O evaporation rate).

We believe that the different microstructures observed stem from the ability/inability of capillary condensed water to remain within and between the silica colloids in the final stages of drying (see Fig. 8). When water does not evaporate from the pores at high humidities, the film has time to condense and gain strength such that when the film is then later transferred to a lower humidity environment, the film does not shrink.

This mechanism is described in more detail for the ethanol-based sols. During spin coating, a film will form and the stagnation point is reached, setting the final dried mass of the coating (see Section 4.1). Ethanol will evaporate at a faster rate than the water due to higher equilibrium ethanol vapor pressure, which results in majority of the liquid in the pores to be water. When water evaporates from the pores it causes capillary pressure (P_c), given by:

$$P_c = \frac{2\gamma \cos\phi}{r_m}. \tag{5}$$

where γ is the surface tension of liquid in the pores (for water is 72×10^{-3} N/m), ϕ is the contact angle of solvent on the colloid surface (for Sol A with water is 20^o), r_m is the mean pore size diameter. The sol-gel derived colloids typically contain a significant amount of microporosity (1-10 Angstroms in size). This has been verified by t-plot analysis from N_2 adsorption measurements (see Table 3) [11].

However, depending on the humidity of the surrounding environment and the pore size, capillary condensed water in the pores can still remain, thus preventing the pores from collapsing. This equilibrium condition is described by the Kelvin equation [17], where the relative humidity (P/P_o= RH) at which a certain size pore can have condensed water is given by:

$$\frac{P}{P_o} = \exp\left(\frac{-2\gamma V_l \cos\phi}{r_m RT}\right) \tag{6}$$

where P is the water vapor pressure (mmHg), P_o is the saturation vapor pressure at temperature (T), and V_l is molar volume of water (18 cm^3/mole). Using Eq. 6, the RH at which condensed water is in equilibrium for a given pore size is plotted in Fig. 9 for ϕ = 20º . The Kevlin equation predicts that all pores less than 10 Å in size would be filled with water for a RH greater 40%. This calculation corresponds reasonably well with the transition RH observed with Sol A (35-40%) in Fig. 1a. If spin coating is performed above this humidity, the water in the pores of the colloids will reach an equilibrium with the atmosphere, and capillary condensed water will remain in the pores of the colloid. With time, silica condensation occurs, and the the film increases in strength. When that coating is then placed in a dry environment, the liquid water is removed from the pores, but the pores do not collaspe due to the strength increase. Hence the coating will shrink less leading to a lower refractive index and thicker coatings. If spin coating is performed below the transition RH, the capillary condensed water will leave the pores. The capillary forces will cause the colloids to collapse and the film to shrink. Hence, the coatings made in low humidities have lower indices and higher thicknesses. The abrupt transition in properties observed in Figs. 1-2 can be explained by the narrow pore distribution present in the colloids (see Table 3).

4.3 Effect of solvent, surface chemistry, and coating method

The sols used in this study differ in solvent, surface chemistry, and coating method. The solvents used clearly impact differences observed (see Fig. 10); ethanol-based sols showed large change in films properties with humidity while the sec-butanol and decane -based sols did not. The three solvents used have very different boiling point (bp) temperatures and water solubility (sol) [ethanol (bp=78^{o}C; sol=infinite), sec-butanol (bp=99.5^{o}C, sol=700 ppm), decane (bp=174^{o}C, sol=0.009 ppm)]. Hence these sols will have different evaporation rates and equilibrium water concentrations which will ultimately impact the concentration of H_2O remaining in the pores. As coating dries, the relative concentrations of the solvents present in the pores of the colloid will change. For ethanol based sols, the ethanol will evaporate at a faster rate than the water, and at the final stages of drying the pores are mostly filled with water. Also, due to the high water solubility, in water vapor will transport into the liquid pores. For the decane based sols, the opposite is true, where decane is mostly present in the pores at the final stages of drying. Finally for the sec-butanol sols, both water and sec-butanol are removed at an equivalent rate, but the final concentration of water in the pores will be low since there was little water in the solvent initially and because of the relatively low water solubility. Hence those sols that had significant water in the pores (namely the ethanol-based sols) are influenced by the humidity in the environment during the final stages of drying.

The surface chemistry of the colloids has been previously measured for most of the sols examined in this study [6] (see Table 1). The Sol E has a hydrophobic surface (trimethylsilyl surface), whereas Sols A and B sols have a hydrophillic surface (silanol surface). Based on the data in Table 2, the surface chemistry does not seem to be the major factor determining if humidity during spin coating can lead to shrinkage of the coatings, because all the Sols showed the effect in ethanol (see Fig. 10).

The surface chemistry does, however, seem to influence magnitude of shrinkage (see Fig. 10). Assuming the pore volume is similar for all the sols, then magnitude of the shrinkage is a function of both the capillary pressure and the strength of the silica matrix. Surface chemistry will undoubtedly influence both of these. Sol E, the hydrophobic sol, will have a higher contact angle thus decreasing capillary pressure (Eq. 5); while at the same time, the trimethylsilyl surface will likely reduce the net amount of condensation that takes place, decreasing the overall strength of the coating. The magnitude of shrinkage (as measured by refractive index change) was largest for Sol E in ethanol solvent, suggesting that decrease in strength (reduced condensation) is the dominent effect.

The surface chemistry also appears to influence the transition humidity. The transition humidity for Sol A and B were quite different (35-40% for Sol A and 25-30% for Sol B). Previous studies [6] found that the surface of Sol B is slightly more hydrophillic than the surface of Sol A (see Table 1), which results in a lower contact angle for Sol B. Lower contact angles shift the equilibrium capillary condensation RH to lower values (see Eq. 6).

The coating method also appears to affect the magnitude of the shrinkage observed. This is clearly illustrated by comparing Fig. 1a with Fig. 2. The dip coated samples had a lower magnitude of shrinkage. These results can be qualitatively explained by the much

lower drying rate during dip coating versus spin coating. At a lower drying rate, the dip coated films have more time for condensation. Hence the films are generally stronger when capillary condense water is removed from the pores, resulting in less overall shrinkage.

4.4 Impact on performance of AR coatings

There are two important considerations of how the influence of humidity during coating will impact the production of AR coatings for NIF. The first one relates to the quality assurance (QA) of the sol-gel solutions. After the synthesis of the solutions, numerous QA measurements are conducted to verify that the sol's properties are acceptable and reproducible [5]. One of the QA measurements is to measure the index and thickness of the sol coating. Based on the results of this study, control of humidity is necessary in order to perform a reproducible QA measurement.

The second, more important, consideration is the potential impact on AR transmission performance of NIF optics. Results have shown that sols in sec-butanol and decane are best suited for coating potassium dihydrogen phosphate (KDP) crystal optics. Therefore the humidity effect should have minimal impact on the reproducibility of KDP AR coatings. The silica optics, on the other hand, are coated with Sol A in ethanol, and all these films are ammonia treated. Fig. 11 shows a contour plot of the transmission through an optic for AR coatings with different indices and thicknesses. The optimal refractive index is between 1.20-1.22 for obtaining the maximum transmission; the optimal thickness is near ~2100 Å. The index data determined for films prepared from Sol A at low and high humidity are designated by dashed lines for before ammonia treatment and by solid lines for after ammonia treatment. Note that the thickness of each coating can be controlled by varying the spin rate, draw rate, or solution concentration. From Fig. 11, we conclude that coating at high humidity should provide for a more optimal AR performance for ammonia treated coatings; an index of 1.18 is better than an index of 1.24. In addition, it is better to design the coating with slightly a lower index since the coating will likely getter some volatile organics during use that will increase the refractive index. Also, the higher humidity coating will have less microcracking and may lead to less optical scatter.

5. Conclusions

The effect of humidity during the spin and dip coating of Stöber silica sols has been characterized and explained. For ethanol-based sols, films prepared at low humidities had a higher refractive index, lower thickness, and greater microcracking than those prepared at high humidities. This change in coating microstructure can be explained by the ability/inability of capillary condensed water in the micropores of the colloid to evaporate prior to achieving full film strength and hence allowing the pores to collapse. The surface chemistry of colloids and coating method were found to influence the magnitude of the shrinkage and humidity of the transition. For sec-butanol and decane -based sols, this relative humidity did not affect film properties because water was not present in the pores in the final stages of drying.

Acknowledgements

Work performed under the auspices of the U.S. DOE by UC, LLNL contract No. W-7405-Eng-48. The authors would like to thank J. Ferreira for performing the SEM work, and A. Burnham, C. Thorsness and J. Fair for helpful discussions. The assistance of M. Suratwala and A. Flammini in the preparation of this manuscript is also greatly appreciated.

References

[1] P. Whitman, et. al. "Improved Antireflection Coatings for the NIF", ICF Quarterly Report: Special Issue: Optics Technology for the National Ignition Facility, UCRL-LR-105821-99- 2, 9 [2] (1999).
[2] J. Murray, SPIE 3492 (Supplement) (1998) 1.
[3] I. M Thomas, "High Damage Threshold Porous Antireflective Coating" Appl. Opt. 25, 1481 (1986).
[4] W. Stöber, A. Fink, E. Bohn, J. Colloid Int. Sci. 26 (1968) 62.
[5] T. Suratwala, L. Carman, "NIF Anti-reflective coating solutions: preparation, procedures, and specifications", LLNL Internal Memo, NIF0053473, 10-12-2000.
[6] T. Suratwala, M. Hanna, E. Miller, P. Whitman, I. Thomas, P. Ehrmann, R. Maxwell, A. Burnham, "Surface Chemistry and Trimethylsilyl Functionalization of Stöber Silica Sols", J. of Non-Cryst. Solids 316 (2003) 349.
[7] C. J. Brinker, et. al., "Sol-Gel Thin Film Formation", Journal of the Ceramic Society of Japan, 99 [10] (1991) 862.
[8] C. J. Brinker, et. al., "Fundamentals of Sol-Gel Dip Coating", Thin Solid Films, 201 (1991) 97.
[9] T. Rehg, B. Higgins, "Spin Coating of Colloidal Suspensions", AlChE Journal, 38 [4] (1992) 489.
[10] S. Gregg, K. Sing, Adsorption, Surface Area, and Porosity, Academic Press, London (1967).
[11] S. Lowell, J. Shields, Powder Surface Area and Porosity, Third Edition, New York: Chapman and Hall (1991) 80.
[12] I. M. Thomas, A. K. Burnham, J. R. Ertel, S.C. Frieders, "Method for reducing the effect of environmental contamination of sol-gel optical coatings", SPIE 3492 (1999) 220.
[13] D. Bornside, C. Macosko, L. Scriven, "On the Modeling of Spin Coating", Journal of Imaging Technology, 13 (1987) 122.
[14] T. Suratwala, et. al., "Control of Porosity in SiO_2:PDMS Polycerams through variations in Sol-Gel Processing and Polymer Content", SPIE 3136 (1997) 36.
[15] C. Brinker, in Access in Nanoporous Materials, T. Pinnavaia, M. Thorpe, Eds. (Plenum Press, New York, 1995) 123-139.
[16] C. Brinker, G. Scherer, "Sol-Gel Science", Academic Press, San Diego (1990).
[17] P. Atkins, Physical Chemistry, 5^{th} Edition, W. H. Freeman and Company, New York (1994) 964.

Table 1: Amount of surface chemical species present on sols in present study[6].

Sol	-OCH_2CH_3 (%)	-SiOH (%)	-$Si(CH_3)_3$ (%)
A	8	93	0
B	2	98	0
D	~70	~30	0
E	~65		~35

Table 2: Refractive index (n) and thickness (t) of various sol coatings spin coated at 14% RH and 60% RH.

Sol	Major Solvent	H_2O content (vol%)	Primary surface	Low humidity spin coat[a]		High humidity spin coat[b]		Difference	
				N	t (nm)	n	t (nm)	Δn	Δt(nm)
A	Ethanol	0.92	-OH	1.206	202	1.164	252	0.042	50
B	Ethanol	1.06	-OH	1.213	187	1.162	230	0.041	43
D	Ethanol	0.25	-OCH_2CH_3	1.197	232	1.168	247	0.029	15
E	Ethanol	*	-$Si(CH_3)_3$	1.221	170	1.154	232	0.067	62
E	Decane	0.96	-$Si(CH_3)_3$	1.213	239	1.214	234	0.001	-5
D	Sec-butanol	*	-OCH_2CH_3	1.201	241	1.200	220	0.001	-20

[a] 14% RH, [b] 60% RH, *not measured

Table 3: BET and T-Plot analysis results from N_2 adsorption isotherms of various air-dried sols.

Sol (air dried)	BET Surface Area (m^2/g)	Micropore Volume (1-10 Å) (cc/g)	Micropore Surface Area (m^2/g)	Macropore Surface Area (m^2/g)
A	611	0.525	494	10
B	548	0.535	466	6
E	437	0.435	435	68
A*	208	0	0	nm

*ammonia vapor treated

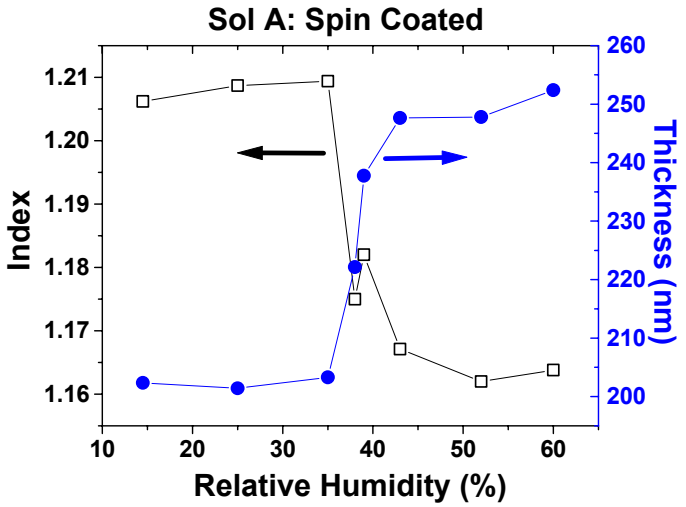

(a)

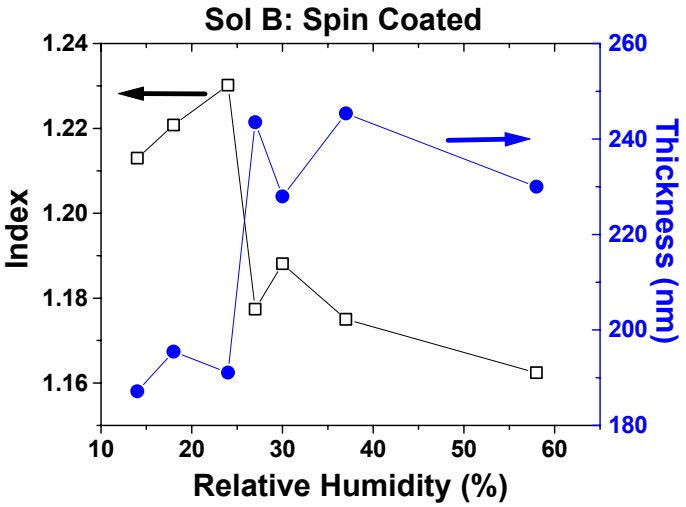

(b)

Figure 1: Refractive index and thickness of films prepared by spin coating at various relative humidities for: (a) Sol A and (b) Sol B.

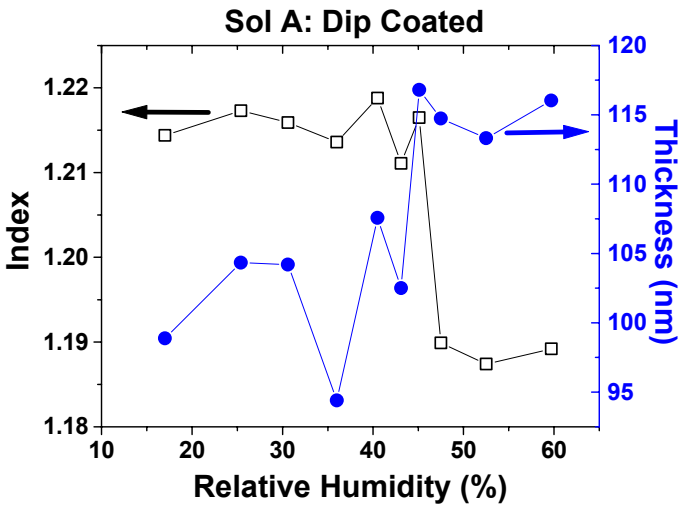

Figure 2. Refractive index and thickness of films prepared by dip coating at various relative humidities for Sol A.

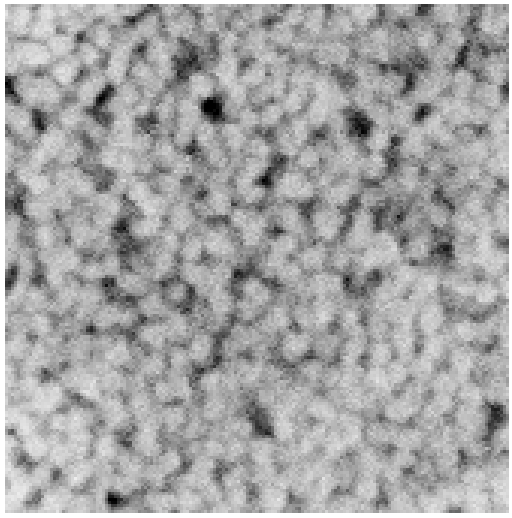

Figure 3: SEM micrograph of the top surface of spin coated Sol A at 52% RH. Full scale is 460 nm; particle size of colloids were measured as ~20nm.

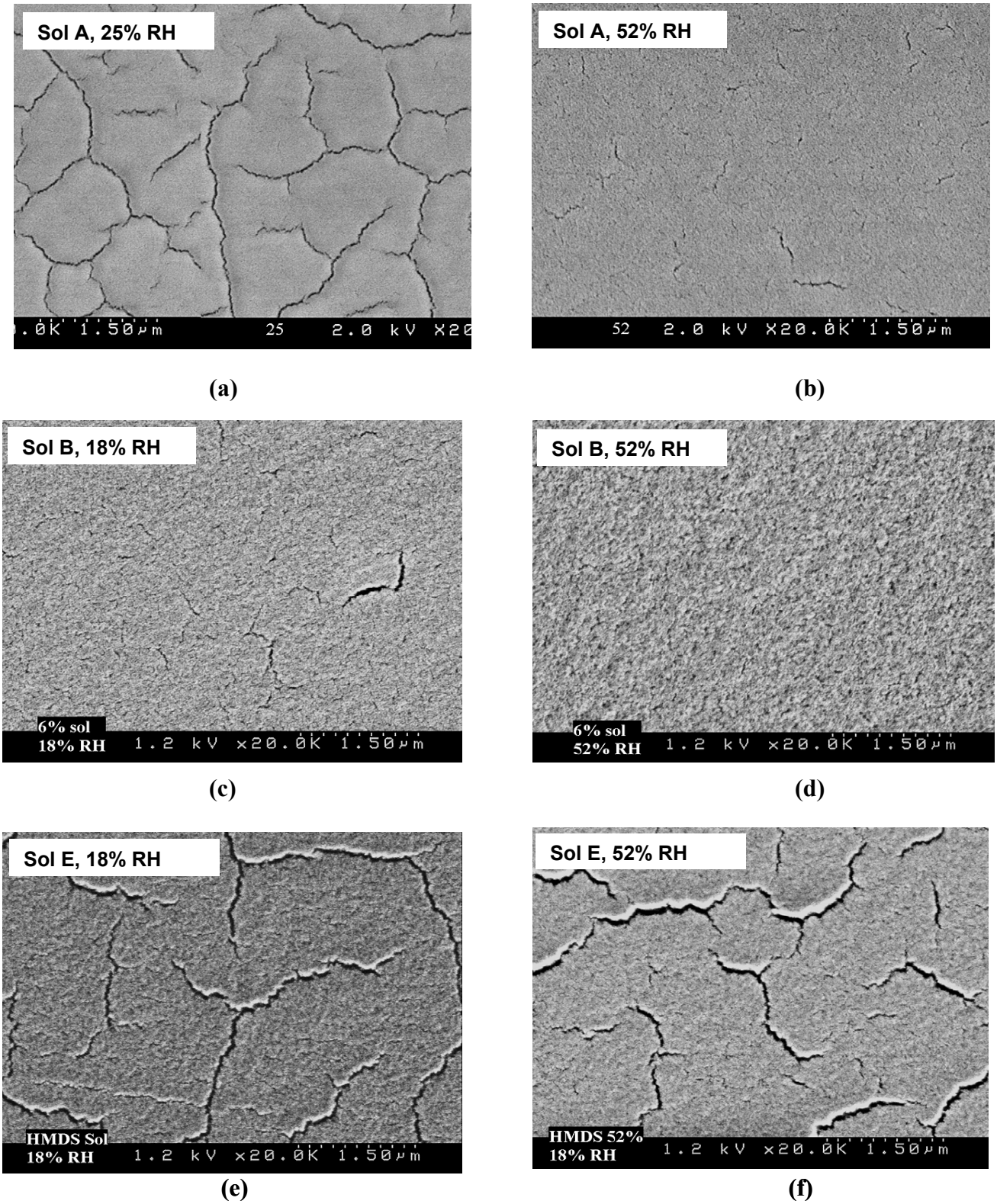

Figure 4: SEM micrographs of the top surface of films from different coating solutions: (a-b) Sol A; (c-d) Sol B; (e-f) Sol E. Images on left are sols coated at low humidities, and images on right are sols coated at high humidities.

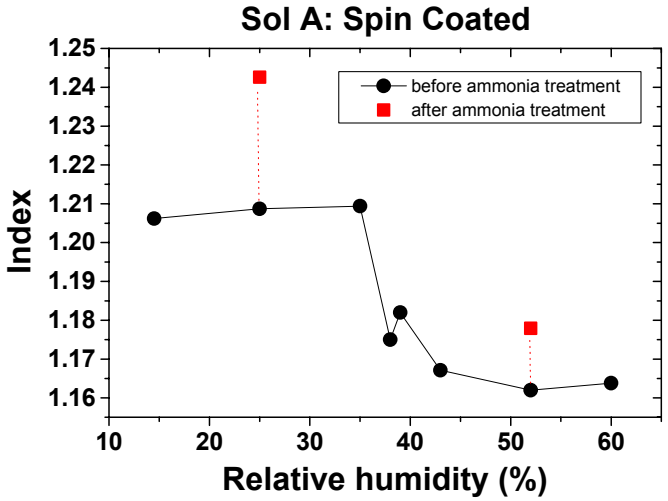

(a)

(b)

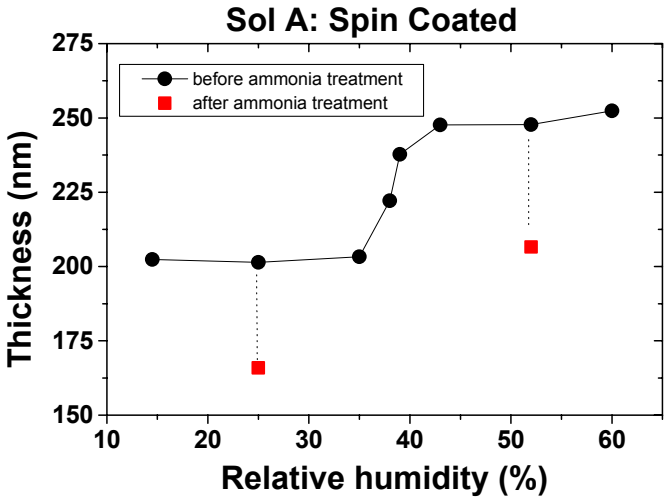

Figure 5: Same as Fig. 1a except that data for ammonia treated samples have been included.

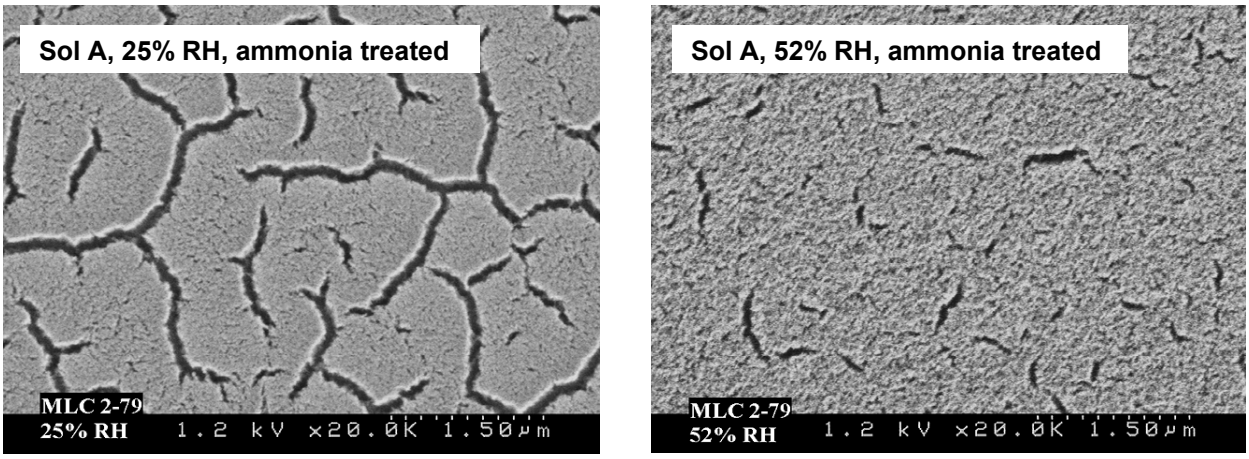

(a) **(b)**

Figure 6: SEM micrographs of the top surface of films (from Sol A) coated at different RHs ((a) 25%, (c) 52%) after a 16 hr ammonia vapor treatment.

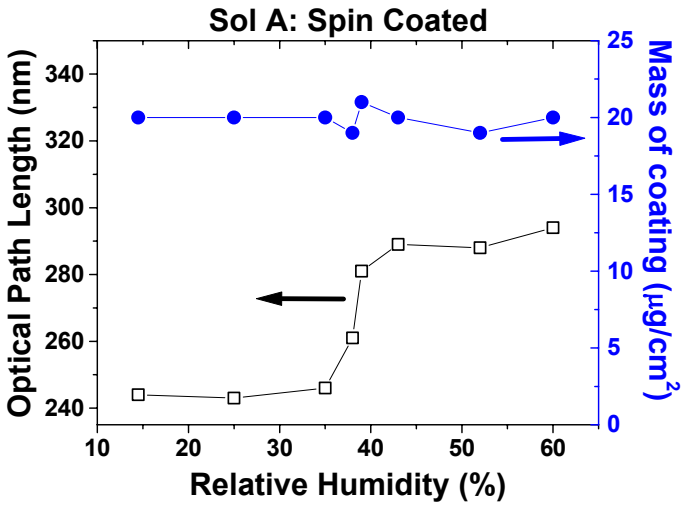

Figure 7: Calculated areal mass of coating (Eqs. 1-2) and OPL (Eq. 3) of Sol A spin coated at various RHs.

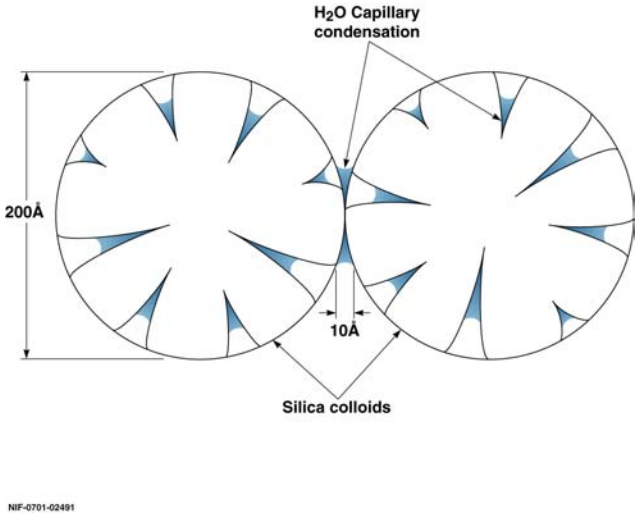

Figure 8: Schematic illustrating water capillary condensation in pores of colloids.

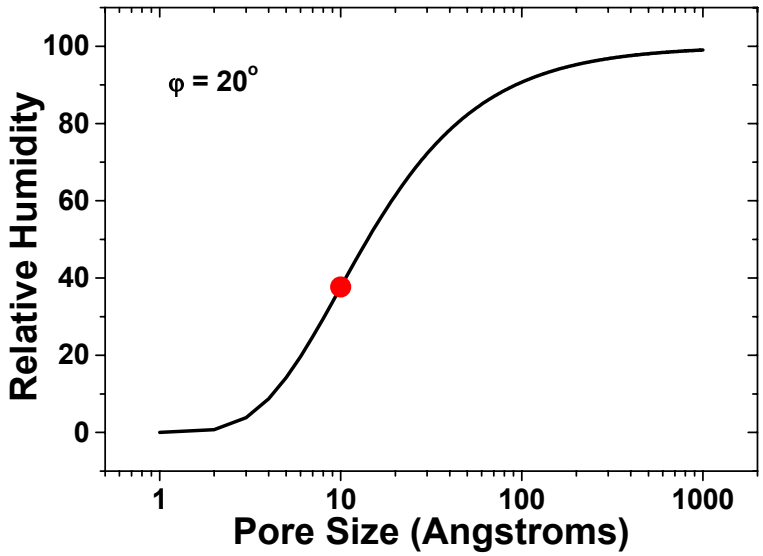

Figure 9: RH at which capillary condensation will occur for various pores sizes at 25°C using Eq. 6. The point represents the RH where a pore size of 10 Å (pores found in sols used in this study) would have water capillary condensation.

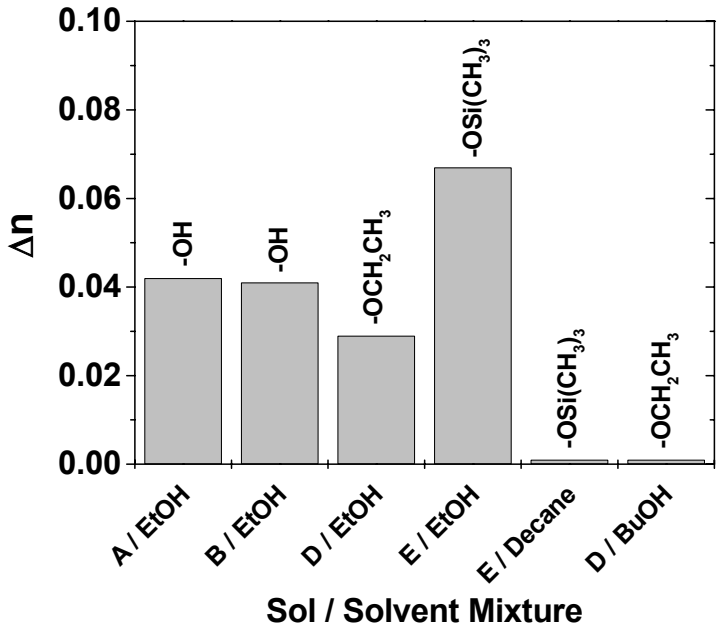

Figure 10: Measured change in refractive index of each sol coating when coated at low humidity vs at high humidity for different sol-solvent mixtures (data reported in Table 2). Primary chemical species on the surface of colloid is labeled above the bar.

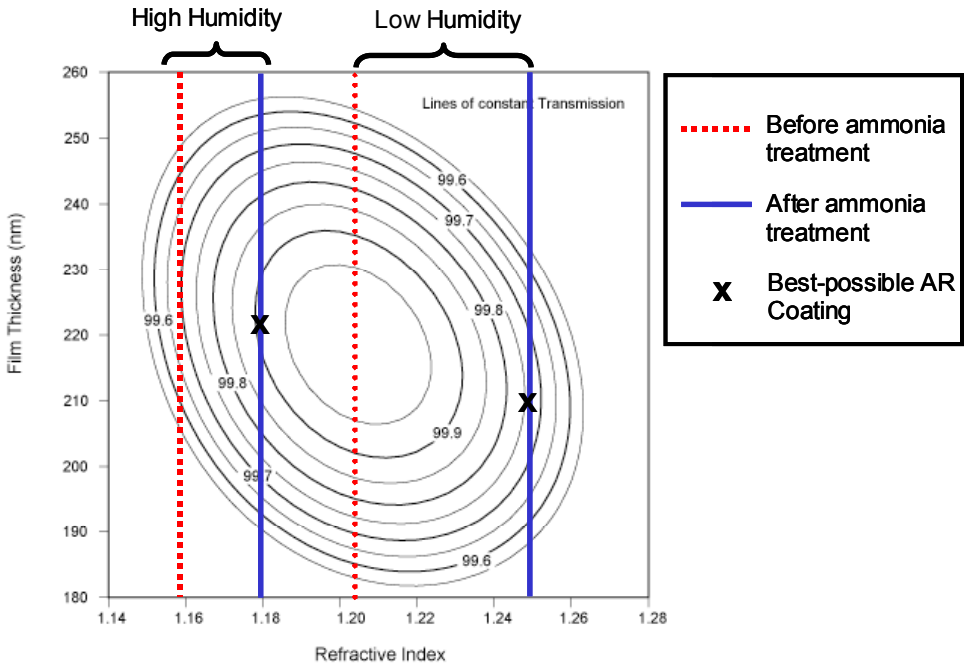

Figure 11: Contour plot of optical transmission (%) at 1.053 nm through an AR coating as a function of index and thickness. The dashed vertical lines represent the index achieved from spin coating Sol A; The solid vertical lines represent the index achieved after vapor ammonia treatment. The points marked by "X" represent the best possible AR coating.

University of California
Lawrence Livermore National Laboratory
Technical Information Department
Livermore, CA 94551